


Molecular characterisation of pancreatic ductal adenocarcinoma with *NTRK* fusions and review of the literature

Michael J Allen ¹, Amy Zhang,² Prashant Bavi,² Jaeseung C Kim,³ Gun Ho Jang,² Deirdre Kelly,¹ Sheron Perera,¹ Rob E Denroche,² Faiyaz Notta,^{2,3} Julie M Wilson,² Anna Dodd,¹ Stephanie Ramotar,¹ Shawn Hutchinson,¹ Sandra E Fischer,⁴ Robert C Grant,^{1,2} Steven Gallinger,^{2,5,6,7} Jennifer J Knox,^{1,2} Grainne M O'Kane^{1,2}

► Additional supplemental material is published online only. To view, please visit the journal online (<http://dx.doi.org/10.1136/jclinpath-2021-207781>).

¹Wallace McCain Centre for Pancreatic Cancer, Princess Margaret Hospital, Toronto, Ontario, Canada

²PanCuRx Translational Research Initiative, Ontario Institute for Cancer Research, Toronto, Ontario, Canada

³Department of Medical Biophysics, University of Toronto, Toronto, Ontario, Canada

⁴Department of Laboratory Medicine and Pathobiology, University of Toronto, Toronto, Ontario, Canada

⁵Hepatobiliary/Pancreatic Surgical Oncology Program, University Health Network, Toronto, Ontario, Canada

⁶Lunenfeld Tanenbaum Research Institute, Mount Sinai Hospital, Toronto, Ontario, Canada

⁷Department of Surgery, University of Toronto, Toronto, Ontario, Canada

Correspondence to

Dr Grainne M O'Kane, Wallace McCain Centre for Pancreatic Cancer, Princess Margaret Hospital, Toronto, ON M5G 2C1, Canada; Grainne.O'Kane@uhn.ca

Received 16 July 2021

Accepted 1 September 2021

Published Online First 28 September 2021



© Author(s) (or their employer(s)) 2023. No commercial re-use. See rights and permissions. Published by BMJ.

To cite: Allen MJ, Zhang A, Bavi P, et al. *J Clin Pathol* 2023;**76**:158–165.

ABSTRACT

Aims The majority of pancreatic ductal adenocarcinomas (PDACs) harbour oncogenic mutations in *KRAS* with variants in *TP53*, *CDKN2A* and *SMAD4* also prevalent. The presence of oncogenic fusions including *NTRK* fusions are rare but important to identify. Here we ascertain the prevalence of *NTRK* fusions and document their genomic characteristics in a large series of PDAC.

Methods Whole genome sequencing and RNAseq were performed on a series of patients with resected or locally advanced/metastatic PDAC collected between 2008 and 2020 at a single institution. A subset of specimens underwent immunohistochemistry (IHC) analysis. Clinical and molecular characterisation and IHC sensitivity and specificity were evaluated.

Results 400 patients were included (resected n=167; locally advanced/metastatic n=233). Three patients were identified as harbouring an *NTRK* fusion, two *EML4-NTRK3* (*KRAS*-WT) and a single novel *KANK1-NTRK3* fusion. The latter occurring in the presence of a subclonal *KRAS* mutation. Typical PDAC drivers were present including mutations in *TP53* and *CDKN2A*. Substitution base signatures and tumour mutational burden were similar to typical PDAC. The prevalence of *NTRK* fusions was 0.8% (3/400), while in *KRAS* wild-type tumours, it was 6.25% (2/32). DNA prediction alone documented six false-positive cases. RNA analysis correctly identified the in-frame fusion transcripts. IHC analysis was negative in the *KANK1-NTRK3* fusion but positive in a *EML4-NTRK3* case, highlighting lower sensitivity of IHC.

Conclusion *NTRK* fusions are rare; however, with emerging therapeutic options targeting these fusions, detection is vital. Reflex testing for *KRAS* mutations and subsequent RNA-based screening could help identify these cases in PDAC.

INTRODUCTION

Pancreatic ductal adenocarcinoma (PDAC) is a leading cause of cancer-related death globally,¹ with a 5-year overall survival (OS) of approximately 10%.² Multiagent chemotherapy remains the mainstay of treatment both in early and advanced disease. In contrast to many other tumour types, targeted approaches are lacking and death rates are not falling.³ Somatic profiling in PDAC, which harbours mutations in Kirsten rat sarcoma (*KRAS*) in 90% of cases, identifies actionable alterations

in only a small number of cases, predominately in *KRAS* wild-type tumours.^{4–8} The frequency of neurotrophic tropomyosin-related kinase (*NTRK*) fusions in pancreatic cancer is estimated at less than 1%,^{9–10} with fusions considered to occur mutually exclusive of other oncogenic drivers including those of the mitogen-activated protein kinase (MAPK) signalling pathway.¹¹

NTRK genes encode a family of genes that are integral to cell proliferation and survival.¹² There are three genes, *NTRK1* (located on chromosome 1q21-q22), *NTRK2* (chromosome 9q22.1) and *NTRK3* (chromosome 15q25) that encode TrkA, TrkB and TrkC, respectively.^{12–14} These genes are physiologically expressed in the central and peripheral nervous system and smooth muscle cells, and overexpressed in some cancers. While *NTRK* mutations were first identified in colorectal and papillary thyroid carcinoma, they are most frequently observed in secretory breast cancer, mammary analogue secretory carcinoma of the salivary glands, as well as some paediatric carcinomas.⁹

Oncogenic fusions occur when the 3' region of the *NTRK* gene binds with the 5' component of fusion partner genes leading to an activated and overexpressed tropomyosin-related kinase, irrespective of the fusion partner.^{11–13} This fusion triggers downstream oncogenic signalling pathways including PI3K-AKT, MAPK and extracellular signal-regulated kinase contributing to cellular proliferation, tumour cell survival, invasion and angiogenesis.^{9–15}

With recent breakthroughs in efficacious treatment targeting *NTRK* fusions including entrectinib and larotrectinib,^{15–16} accurate and timely identification of *NTRK* fusions is paramount. Given the relative rarity of *NTRK* fusions in PDAC as well as there being numerous fusion partners, the current European Society of Medical Oncology (ESMO) guidelines suggest a two-step approach involving screening with immunohistochemistry (IHC) staining followed by next-generation sequencing (NGS) for cases expressing TrkA/B/C.^{11–17} Alternatively, upfront NGS can be performed. The advantage of IHC staining is that it is comparatively quick to obtain results and relatively inexpensive, while global access to NGS can be limited.

We sought to determine the prevalence of *NTRK* fusions in a large series of patients with PDAC. We further explored the clinical and molecular characteristics of patients with these fusions. We compared the sensitivity and specificity of DNA/RNA sequencing and IHC in identifying *NTRK* fusions in PDAC.

MATERIALS AND METHODS

Patient population

In this study, 400 PDAC samples were analysed from patients who underwent surgical resection of a pancreatic adenocarcinoma (n=167) between 2008 and 2015 as previously reported,¹⁸ or were enrolled in the Canadian Comprehensive Molecular Characterization of Advanced Pancreatic Ductal Adenocarcinoma for Better Treatment Selection (COMPASS; a prospective study: NCT02750657) trial (n=233).¹⁹ This trial recruited patients with either a radiological or histological diagnosis of locally advanced or metastatic PDAC. The patients consented to a fresh tumour biopsy, either from the primary tumour or from a metastatic site. Our study includes patients recruited to the COMPASS trial between December 2015 and March 2020. Biopsies and surgical specimens underwent whole genome sequencing (WGS) and RNA sequencing. All samples sequenced were enriched for tumour cells using laser capture microdissection (LCM) and processed as previously described.²⁰ Demographics, treatment and survival outcomes were prospectively collected for both datasets. For the resected cohort of patients, results of WGS/RNAseq were not made available to the patient as this was a retrospective research study.

The study was conducted in accordance to the Declaration of Helsinki regarding clinical trials involving human subjects with additional research ethics board approval obtained from the respective institutional research ethics boards of all institutions involved in the study (University Health Network, Toronto, Ontario, Canada; MUHC Centre for Applied Ethics, Montreal, Quebec, Canada; and Queen's University Health Services and Affiliated Teaching Hospitals Research Ethics Board, Kingston, Ontario, Canada). Each patient consented to participation in the study.

Whole genome sequencing analysis

WGS analysis involved the processing of sequenced reads as previously described^{18 19 21} with single nucleotide variants (SNVs) identified at the intersection of calls by Strelka²² and MuTect.²³ Indels were identified by Strelka.²² Tumour cellularity, ploidy and copy number segments were called by CELLULOID.²¹ Structural variants (SVs) were obtained using the union of outputs from CREST²⁴ and DELLY.²⁵ Mutational signature proportions were calculated using a PDAC-specific subset of v2 COSMIC signatures: 1, 2, 3, 5, 6, 7, 12, 17, 18, 20 and 26.²⁶ Tumour mutational burden (TMB) was calculated by dividing the sum of SNVs and indels over the size of the hg19 reference genome.

Fusion prediction

DNA fusion predictions were made with structural variant tools CREST and DELLY using default parameters. Somatic DNA structural variants detected by these tools with identifiable breakpoints mapped to two different genes were considered to be hypothetical fusions. RNA fusion predictions were made with ericscript and STARfusion using default parameters. These initial fusions were further refined using a minimum of three junction and one spanning fusion-supporting reads as an additional filter.

Fusions predicted from DNA and RNA were combined for downstream analyses.

RNA expression

All 400 patients included had RNAseq data available. PDAC samples can contain an abundance of non-tumour cells/stroma. The relative contribution of this stroma differs between LCM-enriched and bulk sequenced samples. To account for differences in background *NTRK* RNA expression due to tissue of origin, we subdivided RNA sequenced samples into 227 samples from the pancreas and 173 advanced LCM-enriched samples from predominantly liver and other metastatic sites. *NTRK* RNA median expression was derived for these groups separately. Expression fold change values were calculated by normalising each sample's *NTRK* expression against the appropriate median. We then defined samples with *NTRK1/2/3* expression 10 times above the median as samples with *NTRK* RNA overexpression.

Fusion calls

Within our programme, we stratified candidate fusions into three tiers based on levels of evidence supporting a functional fusion. Tier 1 candidates consist of fusions predicted by at least one DNA or RNA fusion caller. Tier 2 candidates have additionally high RNA expression of the *NTRK1/2/3* gene implicated in the fusion. Tier 3 candidates further express an in-frame chimeric transcript containing the *NTRK* kinase domain.

IHC analysis

A subset of patients' specimens with tissue microarrays (TMAs) underwent IHC analysis. IHC staining for TrkA, TrkB and TrkC expressions was performed with the pan-Trk monoclonal antibody clone EPR17341 (Abcam, Cambridge, Massachusetts, USA) validated by Hechtman *et al.*²⁷ The antibody is reactive to a homologous region of TrkA, TrkB and TrkC near the C terminus. Previous positive controls have been identified in cortical brain tissue, ganglia of the colonic plexus submucosa and testis tissue. EPR17341 was used at 6 µ/mL. All assays were performed on a Leica-Bond-3 (Leica, Buffalo Grove, Illinois, USA) automated staining platform using a heat-based antigen retrieval method and high pH buffer solution (ER2, Leica). The negative external controls used were non-neoplastic colorectal and nerve tissue.

Expression patterns of *NTRK*, the percentage of positive tumour cells and staining intensity were reviewed and recorded on all cases. A tumour was scored as pan-Trk IHC positive if there was any (>1+) cytoplasmic and/or nuclear staining identified in the tumour cells. The presence of nerves served as a robust internal positive control in all cases.

Sensitivity and specificity analysis

Sensitivity was determined to be the number of true *NTRK* fusions (based on NGS fusion positivity with an in-frame chimeric transcript—tier 3) divided by the number of cases considered positive for a *NTRK* fusion by IHC. Specificity was defined as the number of true negative cases for *NTRK* fusions divided by the number of cases classified as negative for a *NTRK* fusion.

RESULTS

In this study, 400 patients were sequenced with clinical data available between December 2008 and March 2020. The median age at sequencing was 65.3 years (range 29–87) and 56% were male. Of patients with resected PDAC, the median OS was 20.6 months (95% CI 1.8 to 140.9 months). In patients enrolled

on the COMPASS trial, the median survival was 9.2 months (95%CI 0.3 to 46.1 months). The median TMB was 1.9855 muts/MB across the entire cohort, with the dominant COSMIC signatures identified signature 1 (39.55%), signature 8 (24.32%) and signature 5 (18.81%).

Predicted fusions

Twelve patients (3%) were identified as having at least one DNA/RNA breakpoint in *NTRK* (hypothetical fusion/tier 1 fusion prediction). Four of these 12 (1%) patients had both tier 1 and an upregulation in *NTRK* involved in the breakpoint (tier 2 fusion prediction), while three (0.8%) patients had tier 2 and the *NTRK* predicted fusion in frame with the kinase domain in the correct orientation and intact (tier 3 fusion confirmed). All patients identified as tier 3 were positive for expression of fusion RNA by RT-PCR. The three fusions identified were *EML4-NTRK3* (n=2) and *KANK1-NTRK3* (table 1).

NTRK hypothetical fusions (tier 1)

In the resectable PDAC cohort (n=167), we found 19 hypothetical fusions in 12 patients, with 3 predicted from DNA and RNA, 6 from DNA only and 10 from RNA only (table 2). The majority of the hypothetical fusions were with *NTRK3* (n=12; 63%), while a smaller subset of hypothetical fusions with *NTRK2* (n=5; 26%) and *NTRK1* (n=2; 11%) were identified. We found one recurrent hypothetical fusion, *EML4-NTRK3* (n=2); all other hypothetical fusions were only detected in one sample. In addition, of the 19 hypothetical fusions detected, 16 are novel, with only *EML4-NTRK3* and *PEAR1-NTRK1*²⁸ being previously reported in other cancers.

NTRK RNA overexpression

We evaluated RNA expression two ways: (1) as an alternative independent verification for the presence of *NTRK* fusions (tier 2), and (2) to predetermine fusion false positives by IHC, where RNA overexpression occurs in the absence of a hypothetical fusion. A total of 46 samples were found to have high *NTRK* RNA expression of 10 times or more above the median. *NTRK* RNA overexpression was confirmed for three samples with *NTRK* hypothetical fusions. The remaining 43 samples had high expression in the absence of detectable fusions. RNA overexpression was mutually exclusive between *NTRK1*, 2 and 3.

NTRK fusion characterisation (tier 3)

We analysed the 19 hypothetical fusions with corresponding *NTRK* RNA overexpression for appropriate direction of transcription, preservation of *NTRK* kinase domain and in-frame translation of fusion protein. We found only three fusions, *EML4-NTRK3* (n=2) and *KANK1-NTRK3* (n=1), that met all of these criteria, which we defined as bonafide *NTRK* fusions. *EML4-NTRK3* has been previously reported while *KANK1-NTRK3* has only been described in benign renal metanephric adenomas.²⁹ There were two samples with *EML4-NTRK3* fusions, with both fusions predicted to form the same protein comprised of *EML4* exons 1–6 and *NTRK3* exons 13–20 (figure 1A). The N-terminal *EML4* provides coil–coil domain for downstream signalling, while the C-terminal *NTRK3* provides enzymatic activity through the protein kinase domain. The *KANK1-NTRK3* fusion is similarly comprised of *KANK1* exons 1–7 and *NTRK3* exons 13–20 (figure 1B). Interestingly, *NTRK3* RNA fusion breakpoint is predicted to occur at the same location in all three samples. Tier 1 DNA fusions were associated with six false positives. Of the 400 patients analysed, 32 (8%) were *KRAS* wild-type (16 in

Table 1 Summary of NTRK fusions identified from cohort

	Age at diagnosis (years)	Stage at diagnosis*	Gene	Fusion partner	DNA	RNA	IHC	KRAS	BRAF	GNAS	HRD	MMR	Moffit	OS (months)
Patient 1	80–85	IIA	<i>NTRK3</i>	<i>EML4</i>	Yes	High FC 61	Positive	WT	WT	WT	Intact	Intact	Classic	27.0
Patient 2	55–60	IV	<i>NTRK3</i>	<i>EML4</i>	Yes	High FC 154	–	WT	WT	WT	Intact	Intact	Classic	11.8
Patient 3	70–75	IIB	<i>NTRK3</i>	<i>KANK1</i>	Yes	High FC 27	Negative	G12R mutation	WT	R201H mutation	Intact	Intact	Classic	12.7

*Stage according to AJCC eighth edition.
AJCC, American Joint Committee on Cancer; BRAF, v-raf murine sarcoma viral oncogene homolog B1; FC, fold change; GNAS, guanine nucleotide binding protein, alpha stimulating complex locus; HRD, homologous recombination deficiency; IHC, immunohistochemistry; KRAS, Kirsten rat sarcoma; MMR, mismatch repair; NTRK, neurotrophic tropomyosin-related kinase; OS, overall survival; WT, wild type.

Table 2 Summary of hypothetical tier 1 NTRK fusions identified from cohort

	Age at diagnosis (years)	Stage at diagnosis*	Gene	Fusion partner	DNA	RNA	IHC	KRAS	BRAF	GNAS	HRD	MMR	Moffit	OS (months)
Patient 1	80–85	IIA	NTRK3	EML4	Yes	Yes, high FC 61	Positive	WT	WT	WT	Intact	Intact	Classic	27
Patient 1	80–85	IIA	NTRK3	MTRNR2L12	No	Yes, high FC 61	Positive	WT	WT	WT	Intact	Intact	Classic	27
Patient 2	55–60	IV	NTRK3	EML4	Yes	Yes, high FC 154	–	WT	WT	WT	Intact	Intact	Classic	11.8
Patient 2	55–60	IV	NTRK3	CIB1	No	Yes, high FC 154	–	WT	WT	WT	Intact	Intact	Classic	11.8
Patient 2	55–60	IV	NTRK3	PTPN22	Yes	No, high FC 154	–	WT	WT	WT	Intact	Intact	Classic	11.8
Patient 2	55–60	IV	NTRK3	SEMA4B	Yes	No, high FC 154	–	WT	WT	WT	Intact	Intact	Classic	11.8
Patient 2	55–60	IV	NTRK3	TRIM2	Yes	No, high FC 154	–	WT	WT	WT	Intact	Intact	Classic	11.8
Patient 3	70–75	IIIB	NTRK3	KANK1	Yes	Yes, high FC 27	Negative	G12R mutation	WT	R201H mutation	Intact	Intact	Classic	12.7
Patient 4	66–70	IIIB	NTRK2	NES	No	Yes, low FC 6	–	G12V mutation	WT	WT	Intact	Intact	Classic	14.1
Patient 5	60–65	IIIB	NTRK3	TMEM63A	No	Yes, low FC 4	–	G12D mutation	WT	WT	Intact	Intact	Classic	14.8
Patient 6	70–75	IIA	NTRK3	PCSK6	Yes	No, low FC 0.3	–	G12D mutation	WT	WT	Intact	Intact	Classic	13.6
Patient 7	50–55	IIIB	NTRK2	ATRAID	No	Yes, high FC 72	–	WT	WT	R201H mutation	Intact	Intact	Classic	4.9
Patient 7	50–55	IIIB	NTRK2	LRIG1	No	Yes, high FC 72	–	WT	WT	R201H mutation	Intact	Intact	Classic	4.9
Patient 7	50–55	IIIB	NTRK2	TCEANC2	No	Yes, high FC 72	–	WT	WT	R201H mutation	Intact	Intact	Classic	4.9
Patient 8	55–60	IIIB	NTRK1	PEAR1	No	Yes, low FC 4	–	G12V mutation	WT	WT	Intact	Intact	Classic	3.3
Patient 9	75–80	IIIB	NTRK2	UHRF2	No	Yes, low FC 2	–	G12D mutation	WT	WT	Intact	Intact	Basal-like	22.1
Patient 10	60–65	IV	NTRK3	CHD2	Yes	No, low FC 0	–	G12D mutation	WT	WT	Intact	Intact	Classic	10.1
Patient 11	75–80	IV	NTRK3	NLRP4	Yes	No, low FC 0.1	–	G12V mutation	WT	R524C mutation	Deficient	Intact	Classic	19.5
Patient 12	70–75	IV	NTRK1	PLEC	No	Yes, low FC 0.9	–	G12V mutation	WT	WT	Intact	Intact	Basal-like	2.6

*Stage according to AJCC eighth edition.
AJCC, American Joint Committee on Cancer; BRAF, v-raf murine sarcoma viral oncogene homolog B1; FC, fold change; GNAS, guanine nucleotide binding protein, alpha stimulating complex locus; HRD, homologous recombination deficiency; IHC, immunohistochemistry; KRAS, Kirsten rat sarcoma; MMR, mismatch repair; NTRK, neurotropic tropomyosin-related kinase; OS, overall survival; WT, wild type.

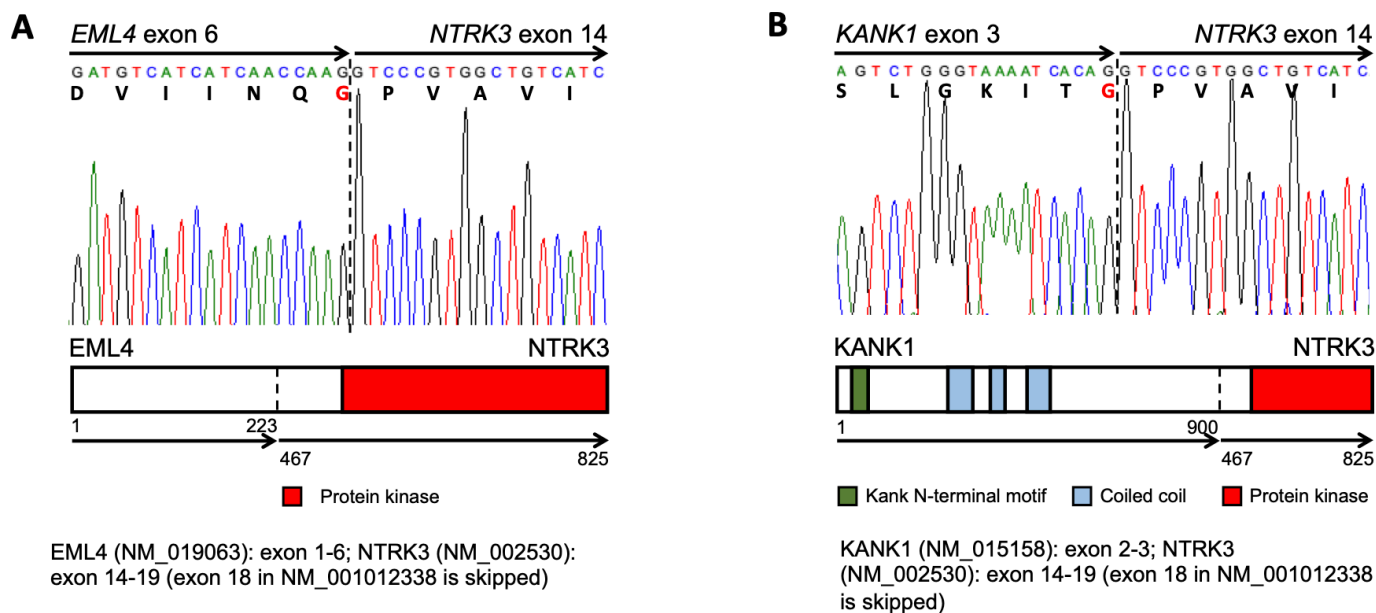


Figure 1 (A, B) RT-PCR validation: (A) Sanger sequencing trace of *EML4-NTRK3* amplified cDNA product from patient 1 and patient 2 tumour RNA. Sequencing trace confirms expression of fusion RNA joining *EML4* exon 6 to *NTRK3* exon 14. The same *EML4-NTRK3* RT-PCR product was detected in patients 1 and 2. A schematic of the putative fusion protein and its conserved domains is shown at the bottom. (B) Sanger sequencing trace of *KANK1-NTRK3* amplified cDNA product from patient 3 tumour RNA. Sequencing trace confirms the expression of fusion RNA joining *KANK1* exon 3 to *NTRK3* exon 14. A schematic of the putative fusion protein and its conserved domains is shown at the bottom.

the resected specimens and 16 patients with metastatic disease). The number of *KRAS* wild-type specimens with a predicted *NTRK* (tier 3) fusion was two (6.25%).

IHC analysis

IHC staining was performed in a subset of 74 resected specimens with TMAs available including two of those with predicted fusions. One case (patient 2) did not have sufficient tissue for IHC analysis. All samples also had DNA and RNA analysis. One of 74 stains was positive (patient 1, figure 2A), with DNA and RNA analysis confirming the presence of an *NTRK* fusion. There were no false-positive IHC stains. One stain was negative despite the presence of an *NTRK* fusion (patient 3, figure 2B). This is attributable to the fusion, *KANK1-NTRK3*, being a plasma membrane fusion. The sensitivity was therefore 50% and specificity 100%, although this must be cautioned in the presence of small numbers.

Patient characteristics

Patient 1

Patient 1 was a male in his early 80s with a resected poorly differentiated pT3N0Mx (stage IIA) PDAC. The patient received adjuvant chemoradiation with gemcitabine, with a disease-free survival (DFS) of 13.9 months and an OS of 27.0 months. The tumour transcriptional phenotype was modified Moffit classical, with DNA prediction positive (figure 3A) and a high RNA fusion fold change (FC) of 61 (figure 3B). Driver mutations identified included *TP53* loss by frameshift (S17fs) with loss of heterozygosity (LOH) and *CDKN2A* homozygous deletion. A *KRAS* oncogenic mutation was not present. The tumour was considered to be proficient in homologous recombination repair (HRP) and mismatch repair (MMRp). Dominant mutational signatures were considered typical (COSMIC signature 1: 50.3%, signature 9: 23.2%, signature 5: 16.9%) (figure 4A). The tumour mutational burden was 2.6 mutations per megabase (mut/Mb).

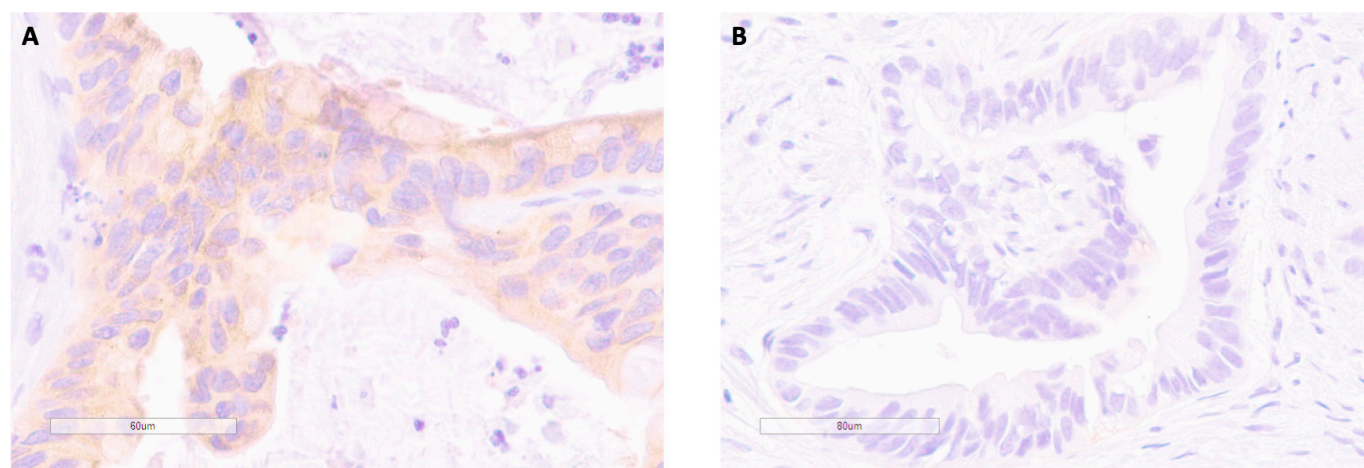


Figure 2 Immunohistochemical staining for patient 1 (A) and patient 3 (B) showing positive and negative staining for TrKA/B/C, respectively.

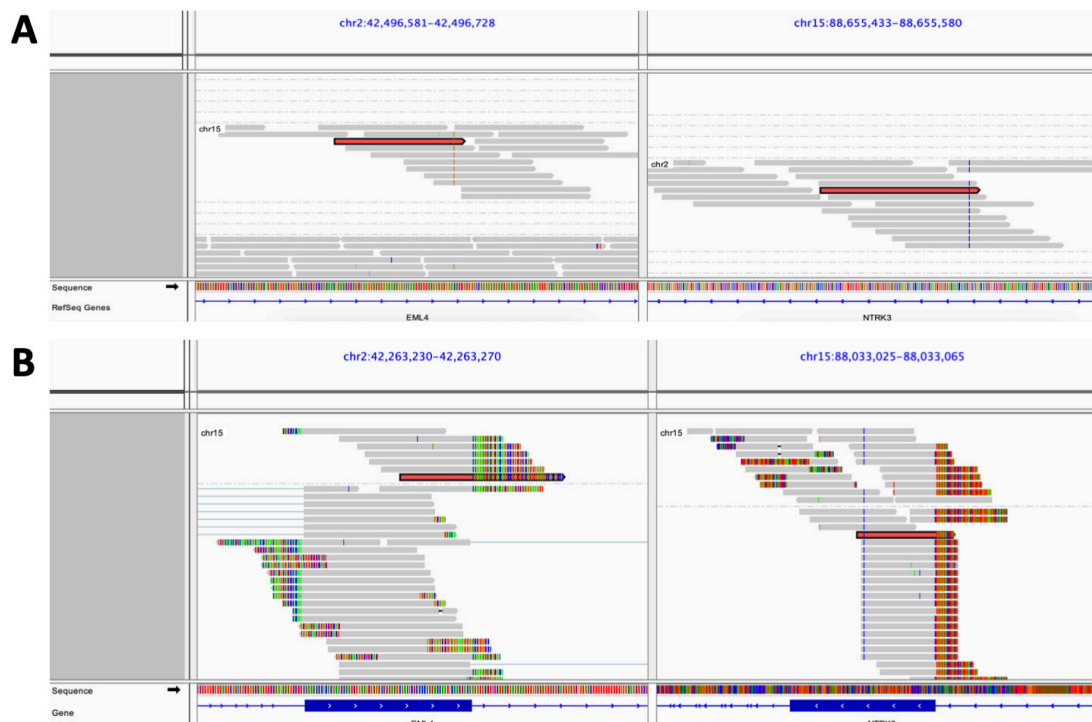


Figure 3 Patient 1: (A) DNA structural variants predicting hypothetical fusion. (B) RNA fusion reads for predicted fusion. (A) Putative *EML4-NTRK3* whole genome sequencing (WGS) fusion reads viewed using IGV (Integrative Genomics Viewer from Broad Institute). WGS reads from tumour were grouped by chromosome. Reads from chr2 at the *EML4* locus are shown on the left and reads from chr15 at the *NTRK3* locus are shown on the right. The two reads highlighted in red are mate pairs which span the *EML4-NTRK3* fusion junction. (B) Putative *EML4-NTRK3* RNA fusion reads viewed using IGV. RNAseq reads were grouped by chromosome. Reads from chr2 at the *EML4* locus are shown on the left and reads from chr15 at the *NTRK3* locus are shown on the right. The two reads highlighted in red are mate pairs which span the *EML4-NTRK3* fusion junction.

A tier 3 bonafide *EML4-NTRK3* fusion was identified. Trk IHC staining was positive (figure 2A).

Patient 2

Patient 2 was a male in his late 50s with metastatic PDAC with synchronous liver metastases. The patient received first-line fluorouracil 2400 mg/m² q46 hour infusion, irinotecan 150 mg/m² and oxaliplatin 85 mg/m² (modified FOLFIRINOX) every 2 weeks with a partial response observed (38% reduction from

baseline). Treatment was discontinued due to progressive disease, with the patient then receiving a novel serine/threonine-protein kinase 4 (PLK4) inhibitor. OS was 11.8 months. The tumour transcriptional subtype was classical, with DNA prediction positive (online supplemental figure 1A) and a high RNA fusion FC of 154 (online supplemental figure 1B). Profiling identified a *KRAS* wild-type tumour with *CDKN2A* and *KDM6A* homozygous deletion. Dominant mutational signatures were typical (COSMIC signature 1: 29.7%, signature 17: 20.6%, signature

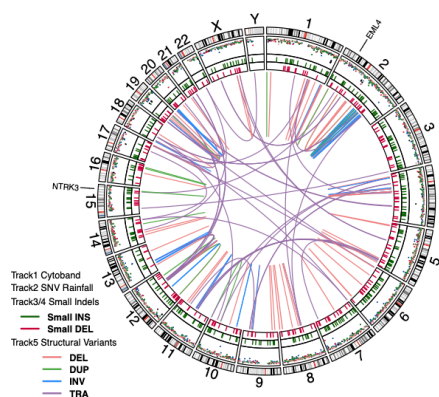


Figure 4A: Patient 1

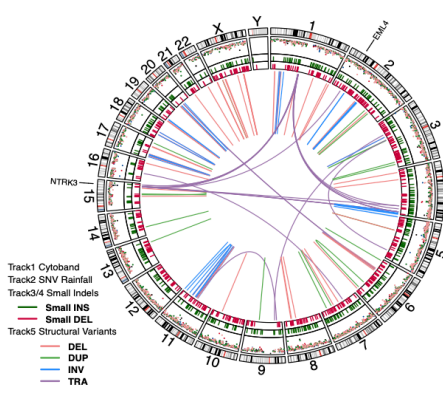


Figure 4B: Patient 2

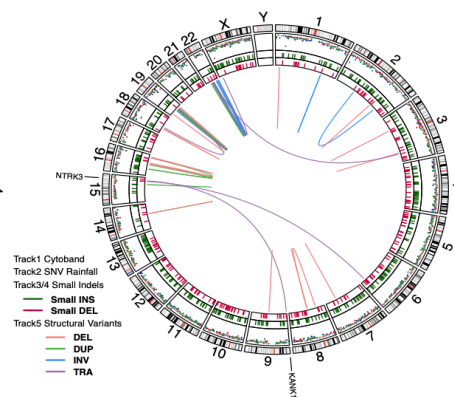


Figure 4C: Patient 3

Figure 4 (A–C) Whole genome plot of tumour for patient 1, patient 2 and patient 3. Features displayed in the Circos plot from outermost to innermost ring are (1) the karyotype ideogram, (2) somatic base substitutions as a rainfall plot (log10 distance between mutations; C>A: blue, C>G: black, C>T: red, T>A: grey, T>A: green, T>G: pink), (3) insertions indicated by short green lines, (4) deletions indicated by short red lines, (5) copy number changes shown as blocks (gain: green, loss: red), and (6) structural variations shown as central lines (duplications: green, deletions: light red, inversions: blue, translocations: violet). *NTRK* and partner fusion genes are labelled around the Circos plot.

8: 20.2%, signature 5: 16.1%) (figure 4B) and the TMB was 4.2 muts/Mb. There was not enough tissue available for IHC testing. A *EML4-NTRK3* fusion was identified; however, this was determined only after the patient had died.

Patient 3

Patient 3 was a female in her early 70s with a resected poorly differentiated pT3N1Mx (stage IIB) PDAC. The patient received adjuvant chemoradiation with gemcitabine. DFS was 10.3 months, with an OS of 12.7 months. The tumour was Moffitt classical, with DNA prediction positive (online supplemental figure 2A) and a high RNA fusion FC of 27 (online supplemental figure 2B). Mutational signatures were typical (COSMIC signature 1: 56.2%, signature 8: 19.8%, signature 5: 14.5%) (figure 4C) and TMB was 2.0 mut/Mb. A subclonal *KRAS G12R* mutation was identified, as well as a *GNAS R210H* mutation. Other driver mutations identified included *TP53* loss by splicing variant (c.277-2A>G) with LOH, *CDKN2A VUS L130P*. IHC in this case was negative (figure 2B). A plasma-membrane *KANK1-NTRK3* fusion was identified.

DISCUSSION

NTRK fusions in PDAC are rare. Similar to other large datasets, the prevalence of *NTRK* fusions in our patient cohort was 0.8% (3/400). We document two fusions in *EML4-NTRK3* in *KRAS* wild-type patients and a novel fusion in *KANK1-NTRK3* in patients with a subclonal *KRAS* mutation. Aside from the absence of a *KRAS* mutation, mutational signatures and tumour mutational burden were similar to that of 'typical' *KRAS*-driven PDAC.

There is notably large heterogeneity in fusion partners, with the oncogenic significance and actionability of those documented in the literature unknown. Fusions previously identified in pancreatic cancer include *CTRC-NTRK1* and *ETV6-NTRK3*.^{6 8 30} *ETV6-NTRK3* is one of the most prevalent *NTRK* fusions and is present in >95% of secretory breast cancers.³¹ *EML4-NTRK3* fusions have previously been described in numerous malignancies while *KANK1* has been described as the fusion partner with *NTRK2* in pilocytic astrocytoma³² and *NTRK3* in benign renal metanephric adenomas. In the former case, the patient did not receive an inhibitor of TRK.

While the prevalence of *NTRK* fusions is low in the total population, the prevalence is much more significant when looking only at the *KRAS* wild-type population, which historically is considered to constitute just 10% of PDAC.⁷ In our population, 32 (8%) of the samples were *KRAS* wild type, with two of these positive for an *NTRK* fusion (6.25%). This strengthens the argument that cascade testing for *KRAS* mutations should be available for all PDAC. In the absence of a *KRAS* mutation, further workup could include *NTRK* IHC and/or expanded NGS testing to determine the presence of fusions including *NTRK* fusions. This consideration is particularly pertinent for health services who do not have the means or financial capacity to perform NGS on all patients with PDAC. Complicating this fact, however, as was apparent in our population, is that subclonal *KRAS*-mutated PDAC can also harbour an *NTRK* fusion. Subclonal *KRAS* have been reported to occur in up to 26% of *KRAS*-mutated lung adenocarcinomas,³³ with the prevalence unknown in PDAC. This suggests that only testing for *NTRK* fusions based on *KRAS* wild type may miss a small, but definite, number of *NTRK* fusion-positive patients. Furthermore, in the case of this novel fusion, the responsiveness to TRK inhibitors is unknown.

Previous publications suggest IHC sensitivity for *NTRK3* is 79.4% and *NTRK1/2* (combined) is 96.6% with 100% specificity in PDAC.³⁴ Our results demonstrate high specificity with lower sensitivity, although our numbers are small and results must be interpreted with caution. Despite this, it does support a high specificity for positive IHC results.

The major limitation to our study is the lack of treatment in those patients with bonafide *NTRK* fusions with TRK inhibitors. There are however case reports and patients with PDAC reported within trials in the literature. Specific to pancreatic cancers, two case reports were identified, one of which describes two patients with a *TPR-NTRK1* fusion treated with entrectinib achieving a partial response³⁵ and a further case report describing a *CTRC-NTRK1* fusion treated with larotrectinib before switching to selitrectinib, with the best radiological response achieved being an initial partial response on larotrectinib.⁶ Additionally, a single patient included in a prospective single-arm basket study of lanotrectinib in solid organ malignancies harboured a *CTRC-NTRK1* fusion and achieved a partial response on treatment.¹⁶ While specific examples of response to TRK inhibitors in pancreatic cancer are few, the observed response in all is promising, and given the scarcity of multiple lines of effective treatments in advanced pancreatic cancers, identifying the few with *NTRK* fusions is paramount, as this increase the number of potential line of systemic therapy.

CONCLUSION

NTRK fusions in pancreatic cancer are rare and not linked to obvious unique clinical features. Reflex testing for *KRAS* mutations followed by RNA sequencing would provide the most accurate mechanism of in-frame fusion detection.

Take home messages

- ⇒ *NTRK* fusions in pancreatic ductal adenocarcinoma (PDAC) are rare, but targetable with novel agents.
- ⇒ It is therefore imperative that they are identified given the relatively few therapeutic options currently available.
- ⇒ The prevalence of *NTRK* fusions is relatively increased in *KRAS* wild-type tumours compared with *KRAS* mutant.
- ⇒ Reflex testing for *KRAS* mutations and subsequent RNA-based screening could help identify *NTRK* fusions cases in PDAC.

Correction notice This article has been corrected since it was published Online First. Author name (Jaeseung C Kim) has been spelled correctly.

Handling editor Runjan Chetty.

Acknowledgements We thank the following individuals who provided patient samples: Gloria M. Petersen, Mayo Clinic College of Medicine, Rochester, MN, USA.

Contributors Study concept and design: MJA and GMO. Data collection and assembly: MJA, AZ, PB, JCK and GMO. Data analysis and interpretation: MJA, AZ and GMO. All authors contributed to manuscript revision. Final approval of manuscript: All authors.

Funding This study was conducted with the support of the Ontario Institute for Cancer Research (PanCuRx Translational Research Initiative) through funding provided by the Government of Ontario (Grant no. I.PANC.998), the Wallace McCain Centre for Pancreatic Cancer supported by the Princess Margaret Cancer Foundation (Grant no. not supplied), the Terry Fox Research Institute (Grant no. 1078), and the Pancreatic Cancer Canada Foundation (Grant no. not supplied). The study was also supported by a charitable donation from the Canadian Friends of the Hebrew University (Alex U. Soyka) (Grant no. 800137). SG is the recipient of an Investigator Award from OICR (Award no. IA-051). We acknowledge the contributions of team members at OICR within the Diagnostic Development platform and the Genomics Program (genomics.oicr.on.ca), as well as the contributions of the University Health Network Oncology Biobank.

Competing interests None declared.

Patient consent for publication Not required.

Ethics approval This manuscript resulted from research approved by the University Health Network, Toronto, Ontario, Canada research ethics review board. The approval ID's are #15-9596 and #08-0767. All participants provided consent before participating in these studies.

Provenance and peer review Not commissioned; externally peer reviewed.

Data availability statement No data are available. No data is available.

Supplemental material This content has been supplied by the author(s). It has not been vetted by BMJ Publishing Group Limited (BMJ) and may not have been peer-reviewed. Any opinions or recommendations discussed are solely those of the author(s) and are not endorsed by BMJ. BMJ disclaims all liability and responsibility arising from any reliance placed on the content. Where the content includes any translated material, BMJ does not warrant the accuracy and reliability of the translations (including but not limited to local regulations, clinical guidelines, terminology, drug names and drug dosages), and is not responsible for any error and/or omissions arising from translation and adaptation or otherwise.

ORCID iD

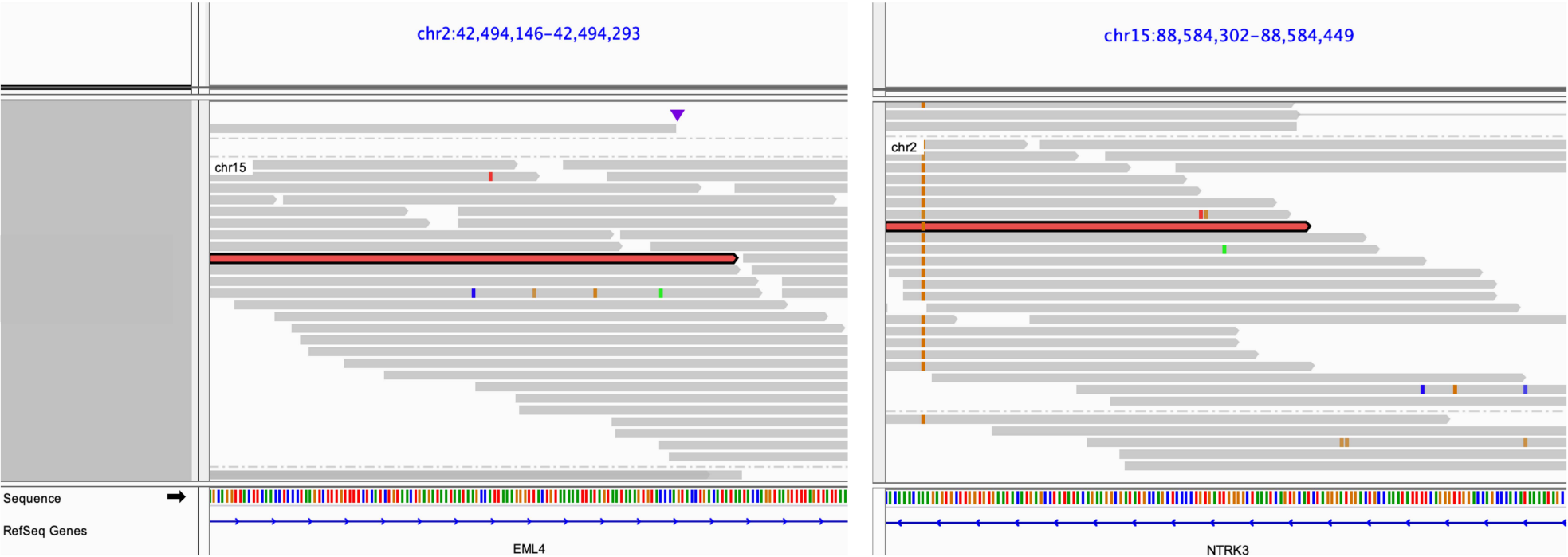
Michael J Allen <http://orcid.org/0000-0001-5091-5995>

REFERENCES

- Bray F, Ferlay J, Soerjomataram I, et al. Global cancer statistics 2018: GLOBOCAN estimates of incidence and mortality worldwide for 36 cancers in 185 countries. *CA Cancer J Clin* 2018;68:394–424.
- Siegel RL, Miller KD, Fuchs HE, et al. Cancer statistics, 2021. *CA Cancer J Clin* 2021;71:7–33.
- Carioli G, Malvezzi M, Bertuccio P, et al. European cancer mortality predictions for the year 2021 with focus on pancreatic and female lung cancer. *Ann Oncol* 2021;32:478–87.
- Singh RR, Goldberg J, Varghese AM, et al. Genomic profiling in pancreatic ductal adenocarcinoma and a pathway towards therapy individualization: a scoping review. *Cancer Treat Rev* 2019;75:27–38.
- Krantz BA, O'Reilly EM. Biomarker-Based therapy in pancreatic ductal adenocarcinoma: an emerging reality? *Clin Cancer Res* 2018;24:2241–50.
- O'Reilly EM, Hechtman JF. Tumour response to Trk inhibition in a patient with pancreatic adenocarcinoma harbouring an NTRK gene fusion. *Ann Oncol* 2019;30:viii36–40.
- Aguirre AJ, Nowak JA, Camarda ND, et al. Real-Time genomic characterization of advanced pancreatic cancer to enable precision medicine. *Cancer Discov* 2018;8:1096–111.
- Lowery MA, Jordan EJ, Basturk O, et al. Real-Time genomic profiling of pancreatic ductal adenocarcinoma: potential Actionability and correlation with clinical phenotype. *Clin Cancer Res* 2017;23:6094–100.
- Cocco E, Scaltriti M, Drilon A. NTRK fusion-positive cancers and Trk inhibitor therapy. *Nat Rev Clin Oncol* 2018;15:731–47.
- Hsiao SJ, Zehir A, Sireci AN, et al. Detection of tumor NTRK gene fusions to identify patients who may benefit from tyrosine kinase (trk) inhibitor therapy. *J Mol Diagn* 2019;21:553–71.
- Marchiò C, Scaltriti M, Ladanyi M, et al. ESMO recommendations on the standard methods to detect NTRK fusions in daily practice and clinical research. *Ann Oncol* 2019;30:1417–27.
- Solomon JP, Hechtman JF. Detection of NTRK Fusions: Merits and Limitations of Current Diagnostic Platforms. *Cancer Res* 2019;79:3163–8.
- Vaishnavi A, Le AT, Doebele RC. TRKING down an old oncogene in a new era of targeted therapy. *Cancer Discov* 2015;5:25–34.
- Zito Marino F, Pagliuca F, Ronchi A, et al. NTRK fusions, from the diagnostic algorithm to innovative treatment in the era of precision medicine. *Int J Mol Sci* 2020;21:3718.
- Amatu A, Sartore-Bianchi A, Siena S. NTRK gene fusions as novel targets of cancer therapy across multiple tumour types. *ESMO Open* 2016;1:e000023.
- Drilon A, Laetsch TW, Kummar S, et al. Efficacy of Larotrectinib in TRK Fusion-Positive Cancers in Adults and Children. *N Engl J Med* 2018;378:731–9.
- Penault-Llorca F, Rudzinski ER, Sepulveda AR. Testing algorithm for identification of patients with Trk fusion cancer. *J Clin Pathol* 2019;72:460–7.
- Connor AA, Denroche RE, Jang GH, et al. Association of distinct mutational signatures with correlates of increased immune activity in pancreatic ductal adenocarcinoma. *JAMA Oncol* 2017;3:774–83.
- Aung KL, Fischer SE, Denroche RE, et al. Genomics-Driven precision medicine for advanced pancreatic cancer: early results from the COMPASS trial. *Clin Cancer Res* 2018;24:1344–54.
- Connor AA, Denroche RE, Jang GH, et al. Integration of genomic and transcriptional features in pancreatic cancer reveals increased cell cycle progression in metastases. *Cancer Cell* 2019;35:267–82.
- Notta F, Chan-Seng-Yue M, Lemire M, et al. A renewed model of pancreatic cancer evolution based on genomic rearrangement patterns. *Nature* 2016;538:378–82.
- Saunders CT, Wong WSW, Swamy S, et al. Strelka: accurate somatic small-variant calling from sequenced tumor-normal sample pairs. *Bioinformatics* 2012;28:1811–7.
- Cibulskis K, Lawrence MS, Carter SL, et al. Sensitive detection of somatic point mutations in impure and heterogeneous cancer samples. *Nat Biotechnol* 2013;31:213–9.
- Wang J, Mullighan CG, Easton J, et al. Crest maps somatic structural variation in cancer genomes with base-pair resolution. *Nat Methods* 2011;8:652–4.
- Rausch T, Zichner T, Schlattl A, et al. DELLY: structural variant discovery by integrated paired-end and split-read analysis. *Bioinformatics* 2012;28:i333–9.
- Alexandrov LB, Nik-Zainal S, Wedge DC, et al. Signatures of mutational processes in human cancer. *Nature* 2013;500:415–21.
- Hechtman JF, Benayed R, Hyman DM, et al. Pan-Trk immunohistochemistry is an efficient and reliable screen for the detection of NTRK fusions. *Am J Surg Pathol* 2017;41:1547–51.
- Lee SJ, Hong JY, Kim K, et al. Detection of fusion genes using a targeted RNA sequencing panel in gastrointestinal and rare cancers. *J Oncol* 2020;2020:1–8.
- Catic A, Kurtovic-Kozaric A, Sophian A, et al. KANK1-NTRK3 fusions define a subset of BRAF mutation negative renal metanephric adenomas. *BMC Med Genet* 2020;21:202–02.
- Demols A, Perez-Casanova L, Rocq L, et al. NTRK gene fusions in bilio-pancreatic cancers. *Journal of Clinical Oncology* 2020;38:e16664–e64.
- Laé M, Fréneaux P, Sastre-Garau X, et al. Secretory breast carcinomas with ETV6-NTRK3 fusion gene belong to the basal-like carcinoma spectrum. *Mod Pathol* 2009;22:291–8.
- López GY, Perry A, Harding B, et al. CDKN2A/B loss is associated with anaplastic transformation in a case of ntrk2 Fusion-positive pilocytic astrocytoma. *Neuropathol Appl Neurobiol* 2019;45:174–8.
- Simon E, Bick T, Sarji S, et al. Clinically significant sub-clonality for common drivers can be detected in 26% of KRAS/EGFR mutated lung adenocarcinomas. *Oncotarget* 2017;8:45736–49.
- Solomon JP, Linkov I, Rosado A, et al. NTRK fusion detection across multiple assays and 33,997 cases: diagnostic implications and pitfalls. *Mod Pathol* 2020;33:38–46.
- Pishvaian MJ, Garrido-Laguna I, Liu SV, et al. Entrectinib in TRK and ROS1 Fusion-Positive Metastatic Pancreatic Cancer. *JCO Precis Oncol* 2018;31:1–7.

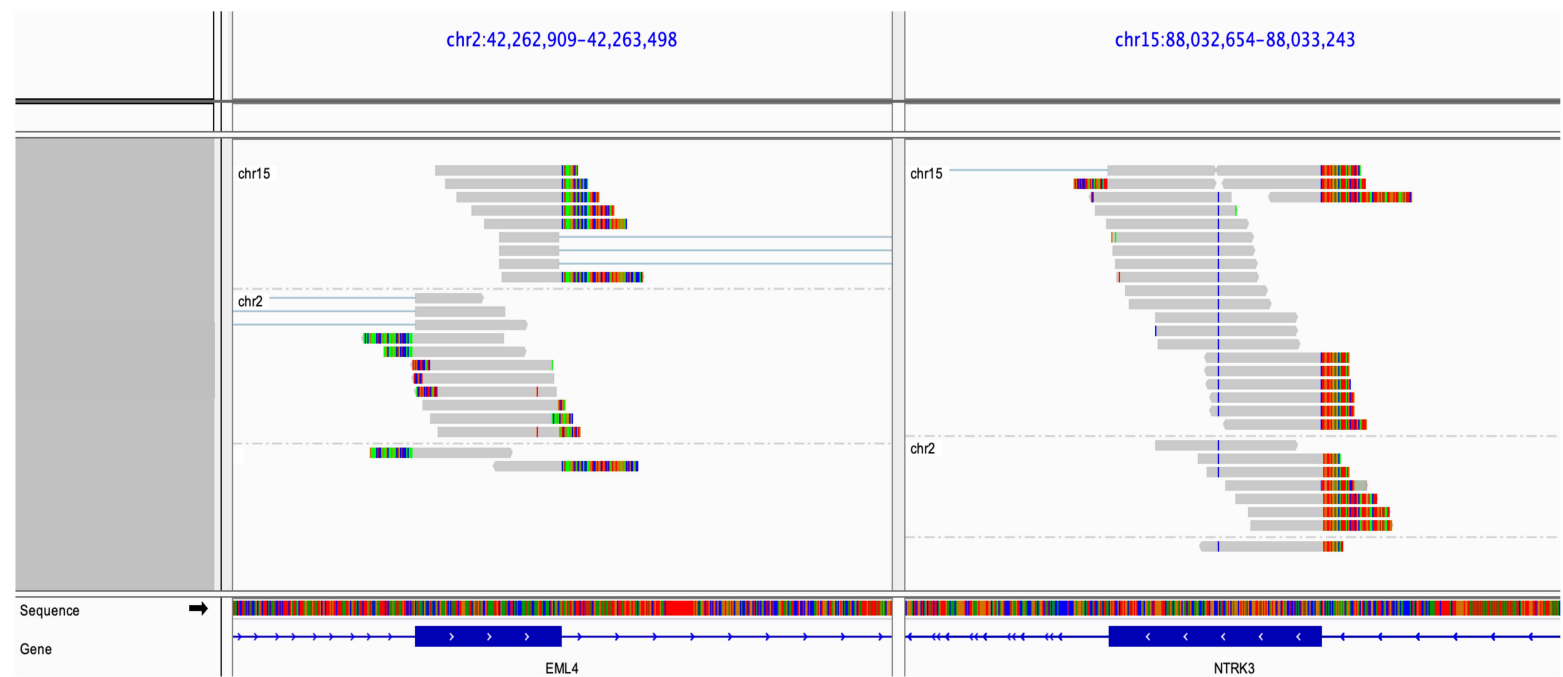
Supplementary Figure 1A: (Patient 2) DNA Structural Variants predicting hypothetical fusion

Putative *EML4-NTRK3* WGS fusion reads viewed using IGV. WGS reads from tumour were grouped by chromosome. Reads from chr2 at the *EML4* locus are shown on the left and reads from chr15 at the *NTRK3* locus, on the right. The two reads highlighted in red are mate pairs which span the *EML4-NTRK3* fusion junction.



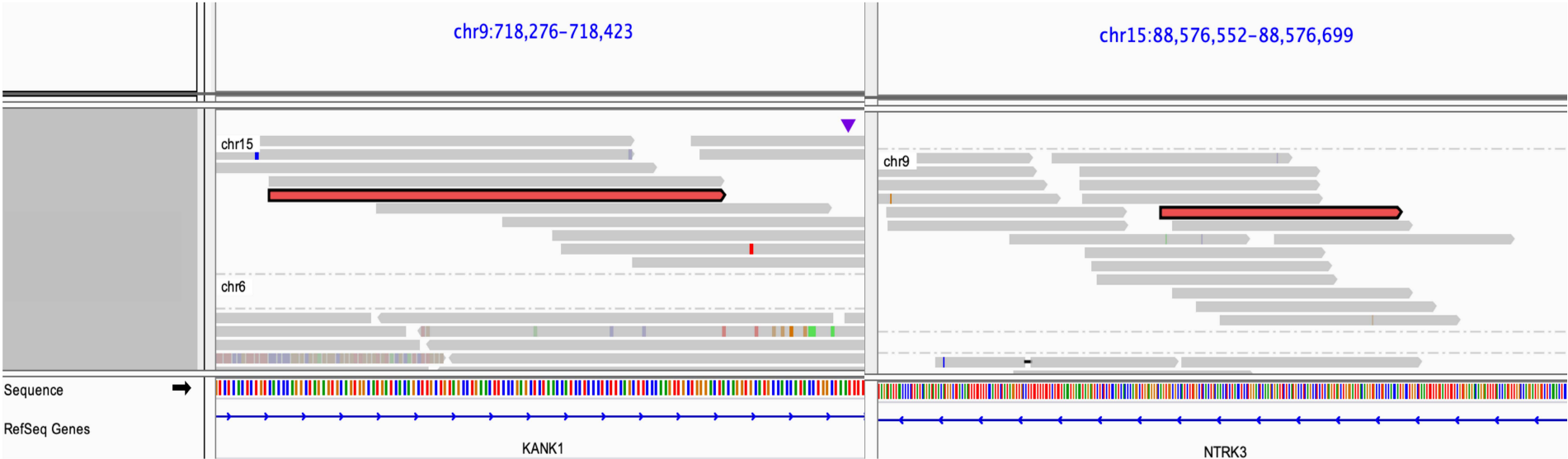
Supplementary Figure 1B: (Patient 2) RNA Fusion Reads for predicted fusion

Putative *EML4-NTRK3* RNA fusion reads viewed using IGV. RNAseq reads from tumour were grouped by chromosome. Reads from chr2 at the *EML4* locus are shown on the left and reads from chr15 at the *NTRK3* locus, on the right. The two reads highlighted in red are mate pairs which span the *EML4-NTRK3* fusion junction.



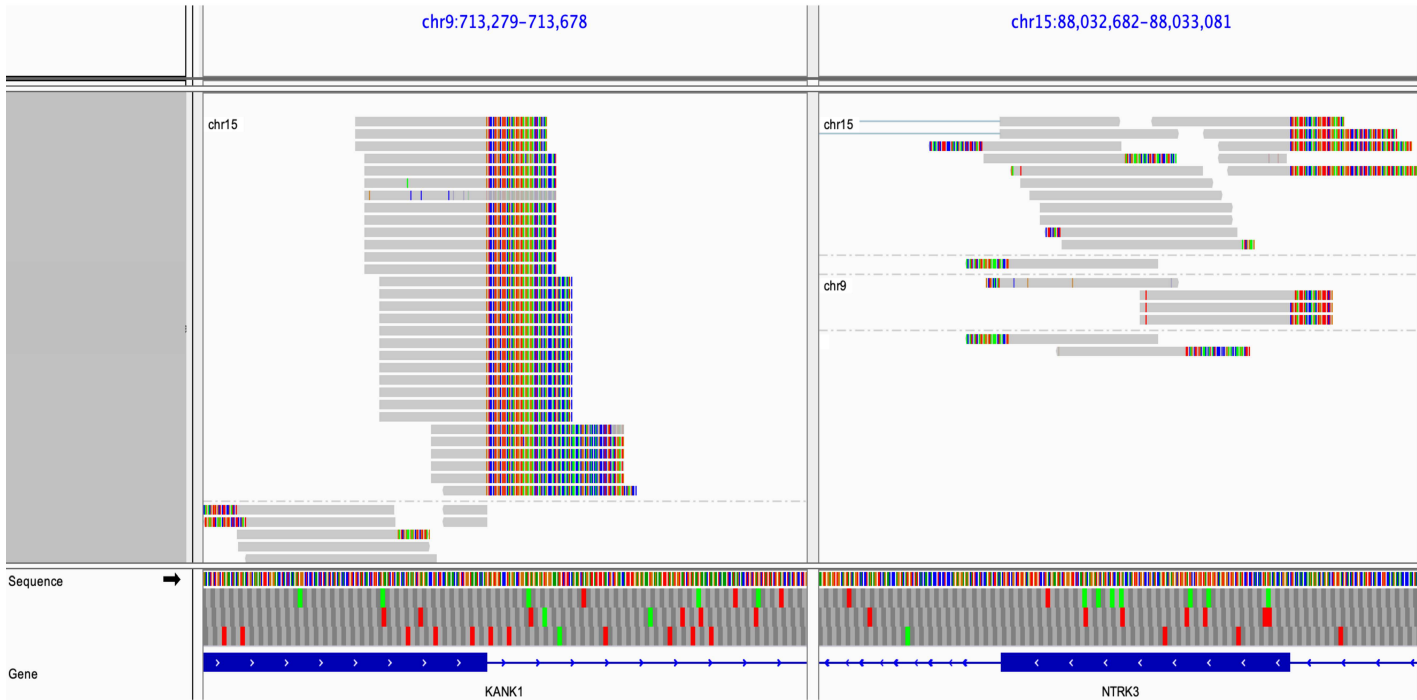
Supplementary Figure 2A: (Patient 3) DNA Structural Variants

Putative *KANK1-NTRK3* WGS fusion reads viewed using IGV. Reads from chr9 at the *KANK1* locus are shown on the left and reads from chr15 at the *NTRK3* locus, on the right. The two reads highlighted in red are mate pairs which span the *KANK1-NTRK3* fusion junction.



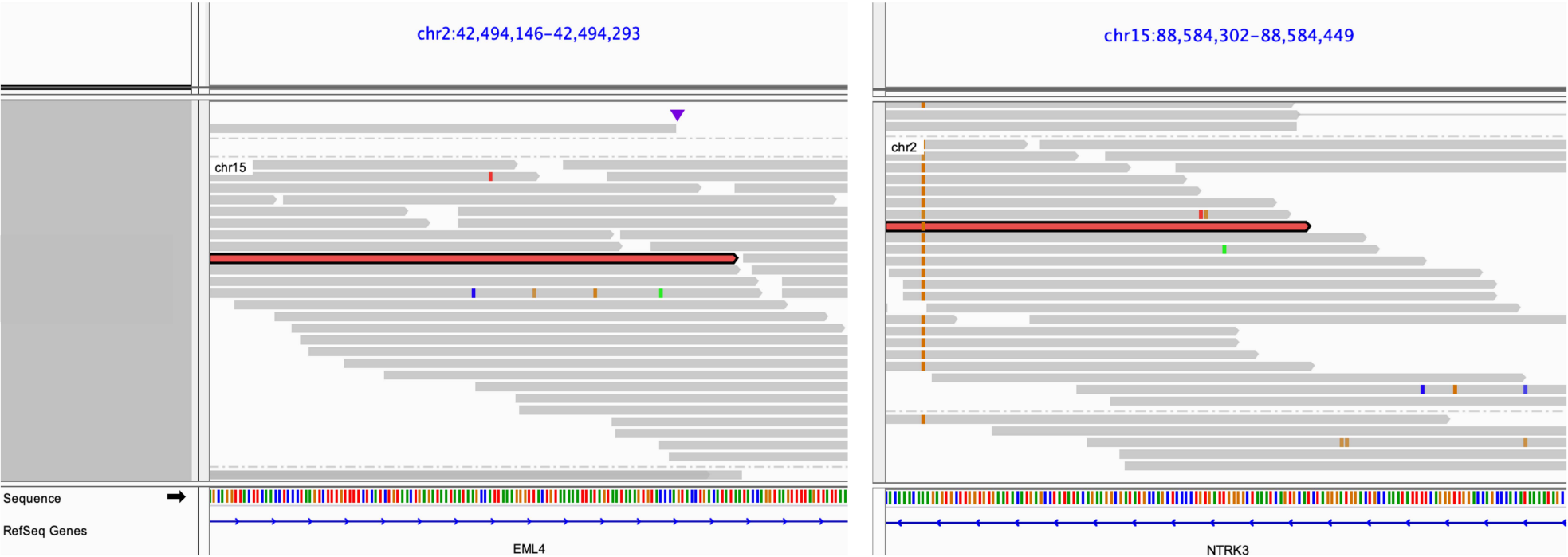
Supplementary Figure 2B: (Patient 3) RNA Fusion Reads

Putative *KANK1-NTRK3* RNA fusion reads viewed using IGV. RNAseq reads from tumour were grouped by chromosome. Reads from chr9 at the *KANK1* locus are shown on the left and reads from chr15 at the *NTRK3* locus, on the right. The two reads highlighted in red are mate pairs which span the *KANK1-NTRK3* fusion junction.



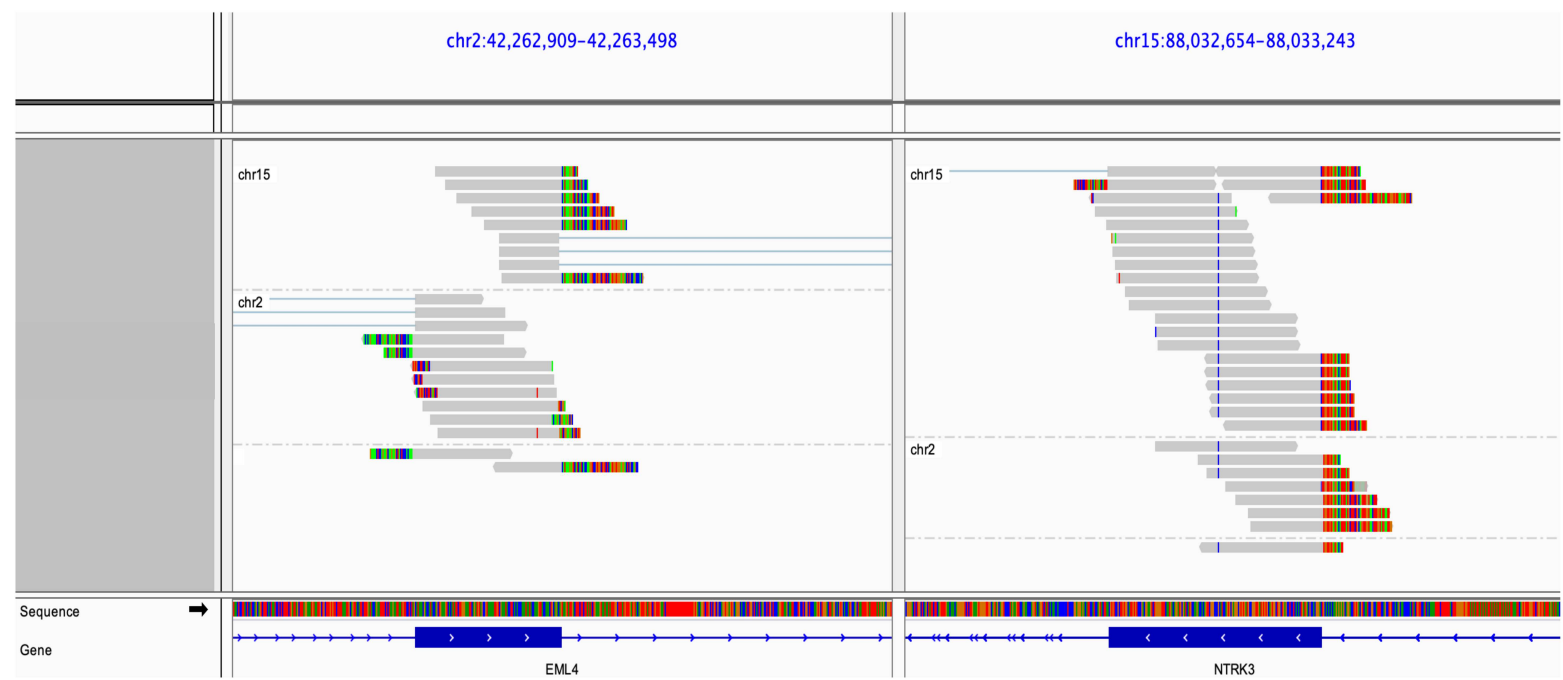
Supplementary Figure 1A: (Patient 2) DNA Structural Variants predicting hypothetical fusion

Putative *EML4-NTRK3* WGS fusion reads viewed using IGV. WGS reads from tumour were grouped by chromosome. Reads from chr2 at the *EML4* locus are shown on the left and reads from chr15 at the *NTRK3* locus, on the right. The two reads highlighted in red are mate pairs which span the *EML4-NTRK3* fusion junction.



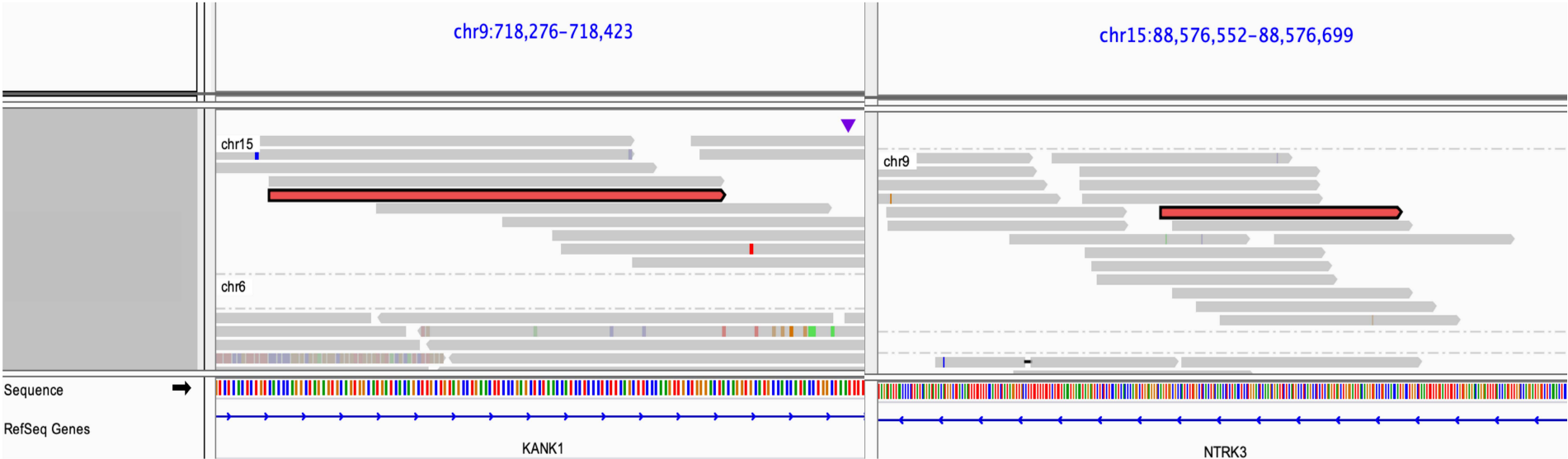
Supplementary Figure 1B: (Patient 2) RNA Fusion Reads for predicted fusion

Putative *EML4-NTRK3* RNA fusion reads viewed using IGV. RNAseq reads from tumour were grouped by chromosome. Reads from chr2 at the *EML4* locus are shown on the left and reads from chr15 at the *NTRK3* locus, on the right. The two reads highlighted in red are mate pairs which span the *EML4-NTRK3* fusion junction.



Supplementary Figure 2A: (Patient 3) DNA Structural Variants

Putative *KANK1-NTRK3* WGS fusion reads viewed using IGV. Reads from chr9 at the *KANK1* locus are shown on the left and reads from chr15 at the *NTRK3* locus, on the right. The two reads highlighted in red are mate pairs which span the *KANK1-NTRK3* fusion junction.



Supplementary Figure 2B: (Patient 3) RNA Fusion Reads

Putative *KANK1-NTRK3* RNA fusion reads viewed using IGV. RNAseq reads from tumour were grouped by chromosome. Reads from chr9 at the *KANK1* locus are shown on the left and reads from chr15 at the *NTRK3* locus, on the right. The two reads highlighted in red are mate pairs which span the *KANK1-NTRK3* fusion junction.

